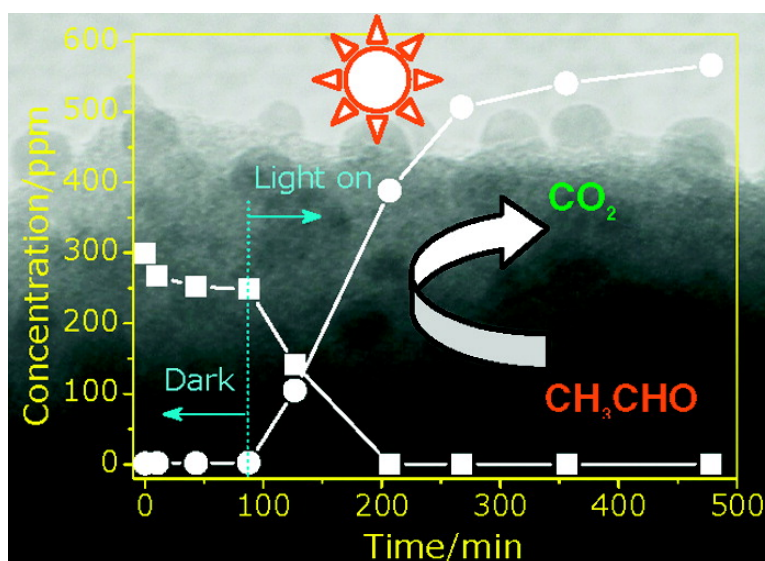## Communication

Efficient Photocatalytic Decomposition of Acetaldehyde over a Solid-Solution Perovskite (AgSr)(NbTi)O under Visible-Light Irradiation

Defa Wang, Tetsuya Kako, and Jinhua Ye

More About This Article

Additional resources and features associated with this article are available within the HTML version:

- Supporting Information
- Links to the 3 articles that cite this article, as of the time of this article download
- Access to high resolution figures
- Links to articles and content related to this article
- Copyright permission to reproduce figures and/or text from this article

View the Full Text HTML

ACS Publications
High quality. High impact.

Efficient Photocatalytic Decomposition of Acetaldehyde over a Solid-Solution Perovskite (Ag$_{0.75}$Sr$_{0.25}$)(Nb$_{0.75}$Ti$_{0.25}$)O$_3$ under Visible-Light Irradiation

Defa Wang,[†] Tetsuya Kako,[‡] and Jinhua Ye*,[†,‡]

International Center for Materials Nanoarchitectonics (MANA), and Photocatalytic Materials Center, National Institute for Materials Science (NIMS), 1-2-1 Sengen, Tsukuba, Ibaraki 305-0047, Japan

Received October 14, 2007; E-mail: jinhua.ye@nims.go.jp

In quest of environmental purification, photocatalysis using semiconductors and sunlight has been attracting tremendous attention. As a green chemistry technology, photocatalysis is an ambient-temperature process that can carry out complete decomposition of organic pollutants at low levels.[1,2] The most extensively studied photocatalyst, TiO_2, possesses a wide band gap ($e_{g(anatase)} \approx 3.2$ eV; $e_{g(rutile)} \approx 3.0$ eV), which can absorb only the UV light accounting for ~4% of the total sunlight to generate charge carriers for promoting the surface redox reactions. This inherent property of TiO_2 restricts its practical applications.

To effectively harvest the visible light that occupies ~43% of the total sunlight, constructing a photocatalysis system with high visible-light activity is indispensable. Since the late 1980s, many efforts have been expended to develop the "second-generation" TiO_2 that can absorb both UV and visible light. Such attempts include (1) photosensitizing with suitable dyes that act as visible-light harvesters but are degraded eventually[3] and (2) doping with transition metal ions[4] or anions (e.g., N, C, and S),[5] which unfortunately act as recombination centers for the photoexcited charge carriers or are simply ineffective in aiding the redox reactions. In recent years, more and more attention has been paid on developing new visible-light-active photocatalysts.[6,7] Among them, the solid-solution semiconductors with tunable electronic structures are of particular interest because of their unique properties that are unattainable by the individual end material.[7]

Recently, we have developed a novel series of perovskite-type solid-solution photocatalysts (Ag$_{1−x}$Sr$_x$)(Nb$_{1−x}$Ti$_x$)O$_3$ crystallized in an orthorhombic ($0 \leq x < 0.9$) or a cubic ($0.9 \leq x \leq 1$) system (Figures S1 and S2, Supporting Information). Preliminary results show that these mixed valent perovskites are powerful for oxidizing H_2O into O_2 from aqueous $AgNO_3$ solution under visible light, and (Ag$_{0.75}$Sr$_{0.25}$)(Nb$_{0.75}$Ti$_{0.25}$)O$_3$ exhibits the best performance. The strong oxidation ability suggests the possibility of photocatalytic decomposition of some organic compounds. Here, we report that acetaldehyde (CH_3CHO), a common indoor air pollutant, can be efficiently decomposed over (Ag$_{0.75}$Sr$_{0.25}$)(Nb$_{0.75}$Ti$_{0.25}$)O$_3$ under visible-light irradiation.

Rietveld refinement shows that (Ag$_{0.75}$Sr$_{0.25}$)(Nb$_{0.75}$Ti$_{0.25}$)O$_3$ is crystallized in an orthorhombic system (space group *Pbcm*) with $a = 5.5653(5)$ Å, $b = 5.5681(5)$ Å, and $c = 15.7263(7)$ Å. The UV−vis spectrum indicates that (Ag$_{0.75}$Sr$_{0.25}$)(Nb$_{0.75}$Ti$_{0.25}$)O$_3$ has an absorption edge at ~440 nm (e_g ~2.8 eV). It should be pointed out that the solid solution (Ag$_{0.75}$Sr$_{0.25}$)(Nb$_{0.75}$Ti$_{0.25}$)O$_3$ is completely different from the mixture of (0.75AgNbO$_3$ + 0.25SrTiO$_3$) (Figures S3−S5, Supporting Information).

Photocatalytic decomposition of CH_3CHO was carried out in a cylindrical static reaction vessel (see details in Supporting Information). Similar to O_2 evolution, the photocatalytic activity of (Ag$_{1−x}$Sr$_x$)(Nb$_{1−x}$Ti$_x$)O$_3$ for decomposition of CH_3CHO into CO_2

also depends on the composition, and the best performance is realized on (Ag$_{0.75}$Sr$_{0.25}$)(Nb$_{0.75}$Ti$_{0.25}$)O$_3$ (see Figure S6, Supporting Information). Figure 1a shows a typical process of photocatalytic decomposition of CH_3CHO into CO_2 over (Ag$_{0.75}$Sr$_{0.25}$)(Nb$_{0.75}$Ti$_{0.25}$)O$_3$ under visible light ($\lambda > 400$ nm). The concentration of initially injected CH_3CHO was ~300 ppm. After keeping the reaction vessel in the dark for ~80 min, the concentration of detectable CH_3CHO was decreased to a nearly unchanged value of ~250 ppm and no CO_2 was evolved, indicating that ~50 ppm CH_3CHO was adsorbed on the catalyst surface. Upon light irradiation, the concentration of detectable CH_3CHO quickly decreased to nearly zero, and the concentration of CO_2 increased linearly. More than 80% of the CH_3CHO was decomposed into CO_2 in the short linear stage. With further increase of irradiation time, the CH_3CHO adsorbed on the catalyst surface was decomposed into CO_2 slowly. Finally, the amount of CO_2 was nearly twice the initial amount of CH_3CHO, i.e., the initially injected CH_3CHO was almost completely decomposed into CO_2, reaching a total carbon balance in the whole reaction. The catalyst was used for several reaction cycles, and its performance was found to repeat very well. XRD, UV−vis, and EDS analyses confirmed that the catalyst was quite stable upon the aforementioned reaction (Figures S7 and S8, Supporting Information).

Using various interference filters (Optical Coatings), the apparent quantum efficiencies of CO_2 evolution were measured and estimated on the basis of the number of incident photons, according to the photooxidation process of CH_3CHO proposed by Fujishima et al.[8] As shown in Figure 1b, the wavelength dependence of quantum efficiency is essentially consistent with the UV−vis spectrum. It is worthy to note that the quantum efficiency of (Ag$_{0.75}$Sr$_{0.25}$)(Nb$_{0.75}$Ti$_{0.25}$)O$_3$ at $\lambda_0 = 440$ nm (1.48%) was over three times that of $TiO_{2−x}N_x$ ($x = 0.0075$) at $\lambda_0 = 436$ nm (0.42%) reported by Asahi et al.,[5a] though the Brunauer−Emmett−Teller (BET) surface area of (Ag$_{0.75}$Sr$_{0.25}$)(Nb$_{0.75}$Ti$_{0.25}$)O$_3$ (~1 m^2 g$^{−1}$) was much smaller than that of $TiO_{2−x}N_x$ (~67 m^2 g$^{−1}$). We expect that the quantum efficiency of our solid solution could be improved significantly by further increasing its surface area.

Photocatalytic decomposition of organics in the presence of O_2 generally involves (1) photoexcitation of electrons from the valence band (VB) to the conduction band (CB); (2) oxidation of organic compound directly via the VB holes or indirectly with the surface-bound hydroxyl radical (•OH); and (3) reduction of O_2 by the CB electrons. Clearly, increased over-potentials, i.e., the difference between VB top potential (H_{vb}) and oxidation potential (H_{ox}) and the difference between CB bottom potential (H_{cb}) and reduction potential (H_{red}), are favorable for the redox reactions. Concerning the visible-light activity of a photocatalyst, a small band gap is equally important.

Usually, the involvement of Ag 4d orbitals moves the VB top of an oxide semiconductor toward the more negative position, while the potential of Nb 4d orbitals is more positive than that of Ti 3d
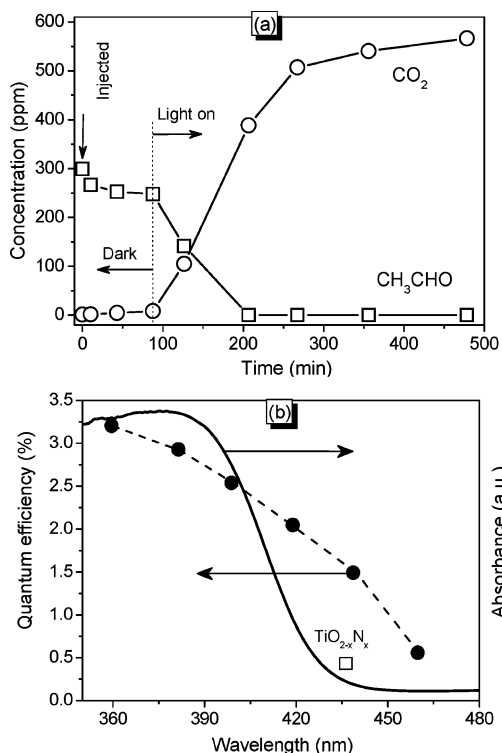
Figure 1. (a) Changes of CH_3CHO and CO_2 concentrations as a function of irradiation time in the presence of $(Ag_{0.75}Sr_{0.25})(Nb_{0.75}Ti_{0.25})O_3$ under visible-light irradiation ($\lambda > 400$ nm). (b) Quantum efficiencies of CO_2 evolution at various light wavelengths, being consistent with the UV−vis absorption spectrum. The quantum efficiency of $TiO_{2-x}N_x$ ($x = 0.0075$) at $\lambda_0 = 436$ nm (0.42%) was cited from Asahi et al.[5a]
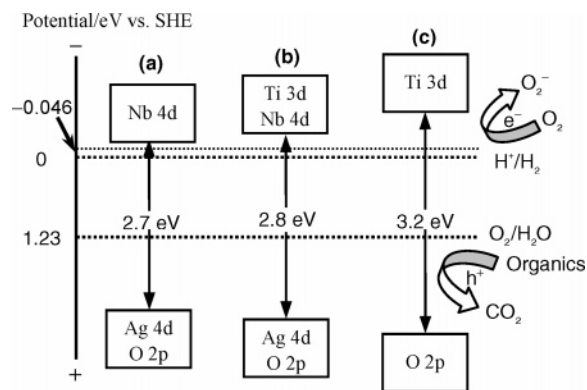

Figure 2. Schematic band structures of (a) $AgNbO_3$, (b) $(Ag_{0.75}Sr_{0.25})(Nb_{0.75}Ti_{0.25})O_3$, and (c) $SrTiO_3$.

orbitals. As a consequence, the band gap of $(Ag_{0.75}Sr_{0.25})(Nb_{0.75}Ti_{0.25})O_3$ is smaller than that of $SrTiO_3$ but larger than that of $AgNbO_3$. On the other hand, the oxidative ability of $(Ag_{0.75}Sr_{0.25})(Nb_{0.75}Ti_{0.25})O_3$ is higher than that of $AgNbO_3$ but lower than that of $SrTiO_3$, while its reductive ability is higher than $AgNbO_3$ but lower than $SrTiO_3$. Figure 2 schematically shows the band structures of $AgNbO_3$, $SrTiO_3$, and $(Ag_{0.75}Sr_{0.25})(Nb_{0.75}Ti_{0.25})O_3$. As a result of its large band gap, $SrTiO_3$ hardly shows visible-light activity, although its CB bottom potential is sufficiently negative (-0.8 eV vs SHE).[9] In contrast, the CB bottom of $AgNbO_3$ is supposed to be very close to H^+/H_2 (0 eV vs SHE) or O_2/O_2^- (-0.046 eV vs SHE), indicating that the over-potential is too small to reduce O_2 by the photoexcited electrons. Therefore, $AgNbO_3$ shows a very low visible-light activity, although its band gap is small. For $(Ag_{0.75}Sr_{0.25})(Nb_{0.75}Ti_{0.25})O_3$, the VB and CB are formed

by the hybridized (Ag 4d + O 2p) orbitals and the hybridized (Ti 3d + Nb 4d) orbitals, respectively, and are supposed to disperse continuously in a relatively wide energy range. This configuration is obviously favorable for the charge carrier transportation. Taking into account the band edges of $SrTiO_3$ and $AgNbO_3$, we assign the CB bottom and VB top of $(Ag_{0.75}Sr_{0.25})(Nb_{0.75}Ti_{0.25})O_3$ around -0.2 and 2.6 eV (vs SHE), respectively. In no doubt, a good compatibility between the absorbance of visible light and the redox abilities has been obtained in $(Ag_{0.75}Sr_{0.25})(Nb_{0.75}Ti_{0.25})O_3$ with a modulated band structure, thus giving rise to a significantly enhanced photocatalytic activity for CH_3CHO decomposition. In addition, another popularly used model organic pollutant, 2-proponal, could also be degraded efficiently over the reported solid-solution photocatalyst under visible-light irradiation.

In summary, we have successfully developed a novel highly active solid-solution photocatalyst $(Ag_{0.75}Sr_{0.25})(Nb_{0.75}Ti_{0.25})O_3$ for efficient decomposition of organic pollutants under visible-light irradiation. The enhanced photocatalytic activity of $(Ag_{0.75}Sr_{0.25})(Nb_{0.75}Ti_{0.25})O_3$ is attributed to the modulated band structure formed by a hybrid conduction band of the empty (Ti 3d + Nb 4d) orbitals and a hybrid valence band of the occupied (O 2p + Ag 4d) orbitals. The present study proves that making solid-solution oxides is a feasible approach for developing highly visible-light-active semiconductor photocatalysts.

Supporting Information Available: Experimental procedures for material preparation, characterization, and photocatalytic activity evaluation. Rietveld refinement results of $(Ag_{1-x}Sr_x)(Nb_{1-x}Ti_x)O_3$. CO_2 evolution rates as a function of the x-value in $(Ag_{1-x}Sr_x)(Nb_{1-x}Ti_x)O_3$. Activities of $(Ag_{0.75}Sr_{0.25})(Nb_{0.75}Ti_{0.25})O_3$, $AgNbO_3$, $SrTiO_3$, ($0.75AgNbO_3 + 0.25SrTiO_3$), and TiO_2 (anatase) under various irradiations. XRD, UV−vis, and/or EDS of $AgNbO_3$, $SrTiO_3$, ($0.75AgNbO_3 + 0.25SrTiO_3$), and $(Ag_{0.75}Sr_{0.25})(Nb_{0.75}Ti_{0.25})O_3$ before and after reaction. This material is available free of charge via the Internet at http://pubs.acs.org.

References

(1) (a) Hoffmann, M. R.; Martin, S. T.; Choi, W.; Bahnemann, D. W. *Chem. Rev.* **1995**, *95*, 69−96. (b) Linsebigler, A. L.; Lu, G. Q.; Yates, J. T. *Chem. Rev.* **1995**, *95*, 735−758. (c) Fujishima, A.; Hashimoto, K.; Watanabe, T. *TiO₂ Photocatalysis: Fundamentals and Applications*; BKC Inc.: Tokyo, Japan, 1999; pp 80−114.
(2) (a) Falconer, J. L.; Magrini-Bair, K. A. *J. Catal.* **1998**, *179*, 171−178. (b) Tao, X.; Ma, W.; Zhang, T.; Zhao, J. *Angew. Chem., Int. Ed.* **2001**, *40*, 3014−3016. (c) Serpone, N. *J. Phys. Chem. B* **2006**, *110*, 24287−24293.
(3) (a) O'Regan, B.; Gratzel, M. *Nature* **1991**, *353*, 737−740. (b) He, J.; Benkö, G.; Korodi, F.; Polívka, T.; Lomoth, R.; Åkermark, B.; Sun, L.; Hagfeldt, A.; Sundström, V. *J. Am. Chem. Soc.* **2002**, *124*, 4922−4932.
(4) (a) Herrmann, J. M.; Disdier, J.; Pichat, P. *Chem. Phys. Lett.* **1984**, *108*, 618−622. (b) Rodrigues, S.; Ranjit, K. T.; Uma, S.; Martyanov, I. N.; Klabunde, K. J. *Adv. Mater.* **2005**, *17*, 2467−2471.
(5) (a) Asahi, R.; Morikawa, T.; Ohwaki, T.; Aoki, K.; Taga, Y. *Science* **2001**, *293*, 269−271. (b) Khan, S. U. M.; Al-Shahry, M.; Ingler, W. B. *Science* **2002**, *297*, 2243−2245. (c) Sakthivel, S.; Kisch, H. *Angew. Chem., Int. Ed.* **2003**, *42*, 4908−4911.
(6) (a) Zou, Z.; Ye, J.; Sayama, H.; Arakawa, H. *Nature* **2001**, *414*, 625−627. (b) Tang, J.; Zou, Z.; Ye, J. *Angew. Chem., Int. Ed.* **2004**, *43*, 4463−4466.
(7) (a) Tsuji, I.; Kato, H.; Kobayashi, H.; Kudo, A. *J. Am. Chem. Soc.* **2004**, *126*, 13406−13413. (b) Yao, W.; Ye, J. *J. Phys. Chem. B* **2006**, *110*, 11188−11195. (c) Maeda, K.; Teramura, K.; Lu, D.; Takata, T.; Saito, N.; Inoue, Y.; Domen, K. *Nature* **2006**, *440*, 295−295.
(8) (a) Sopyan, I.; Watanabe, M.; Murasawa, S.; Hashimoto, K.; Fujishima, A. *J. Photochem. Photobiol., A* **1996**, *98*, 79−86. (b) Ohko, Y.; Tryk, D. A.; Hashimoto, K.; Fujishima, A. *J. Phys. Chem. B* **1998**, *102*, 2699−2704.
(9) Xu, Y.; Schoonen, M. A. A. *Am. Mineral.* **2000**, *85*, 543−556.

JA710805X